Published OnlineFirst August 20, 2012; DOI: 10.1158/1078-0432.CCR-11-2947

Table 1. Characteristics of subjects positive for *EML4-ALK* by the RT-PCR diagnostic system.

Identification number	Sex/ age, y	Pathologic classification	Specimen type	*EML4-ALK* variant	Smoking history (pack-years)	TNM classification	Clinical stage	iAEP	*EGFR* mutation	*KRAS* mutation
J-#1	M/27	Adenocarcinoma	Sputum (2 different time points)	E13;A20	0	cT4N3M1	4	+	–	–
J-#4	F/39	Adenocarcinoma	Metastatic lymph node	E20;A20	NA	cTxN3M1	4	+	–	–
J-#7	M/74	Adenocarcinoma	Bronchial washing fluid	E13;A20	50	cT4N3M1	4	ND	–	–
J-#12	F/56	Adenocarcinoma	Resected tumor	E13;A20	0	cT1N0M0	1A	+	–	ND
J-#53	M/48	Adenocarcinoma	Tumor biopsy/sputum	E13;A20	0	cT3N2M1	4	+	–	–
J-#88	F/37	Adenocarcinoma	Pleural effusion	E13;A20	0	cT4N3M1	4	ND	–	–
J-#127	F/49	Adenocarcinoma	Tumor biopsy	E6a/b;A20	0.9	cT1N2M1	4	+	–	–
J-#189	F/37	Adenocarcinoma	Resected tumor	E14::ins2; ins56A20	0	cT2N1M1	4	+	–	–
J-#210	F/37	Adenocarcinoma	Resected tumor	E13;A20	0	cT4N2M1	4	ND	–	–
J-#215	F/61	Adenocarcinoma	Sputum	E13;A20	82	cT4N2M1	4	ND	–	–
J-#330	M/72	Adenocarcinoma	Pleural effusion/resected tumor (2 different regions)	E13;A20	0	cT4N1M1	4	+	–	–
J-#350	F/53	Adenocarcinoma	Pleural effusion	E13;A20	0	cT4N2M0	3B	ND	–	–
J-#378	F/78	Adenocarcinoma	Resected tumor	E13;A20	0	cT1N0M0	1A	ND	–	–
J-#385	F/80	Adenocarcinoma	Pleural effusion	E6a/b;A20	0	cT4N3M1	4	ND	–	–
J-#391	F/55	Adenocarcinoma	Tumor biopsy	E13;A20	16.5	cT2N2M1	4	+	–	ND
J-#392	F/38	Adenocarcinoma	Tumor biopsy	E13;A20	34	cT4N2M0	3B	+	–	ND
J-#393	F/42	Adenocarcinoma	Tumor biopsy	E13;A20	0	cT4N3M1	4	–	–	ND
J-#409	F/35	Adenocarcinoma	Tumor biopsy	E13;A20	0	cT4N0M0	3B	+	–	–
J-#422	M/69	Adenocarcinoma	Tumor biopsy	E6a/b;A20	0	cT2N2M0	3A	ND	–	–
J-#450	F/30	Adenocarcinoma	Bronchial washing fluid	E6a/b;A20	0	cT4N2M1	4	+	–	–
J-#530	F/55	Adenocarcinoma	Bronchial washing fluid	E13;A20	0	cT1N1M1	4	+	+	ND
J-#646	F/36	Adenocarcinoma	Bronchial washing fluid	E6a/b;A20	0	cT2N3M0	3B	ND	–	–
J-#657	F/62	Adenocarcinoma	Bronchial washing fluid	E13;A20	15	cT4N2M0	3B	ND	–	–
J-#759	F/32	Adenocarcinoma	Resected tumor	E13;A20	12	cT1N0M0	1A	ND	–	–
J-#771	M/32	Adenocarcinoma	Tumor biopsy	E6a/b;A20	15	cT1N3M1	3B	ND	–	–
J-#817	M/33	Adenocarcinoma	Pleural effusion	E13;A20	0	cT2N1M1	4	ND	–	–
J-#848	M/57	Adenocarcinoma	Bronchial washing fluid	E18;E20	0	cT4N2M0	3B	ND	–	–
J-#887	F/32	Adenocarcinoma	Bronchial washing fluid	E6a/b;A20	0	cTxN3M1	4	ND	–	ND
J-#927	M/36	Adenocarcinoma	Bronchial washing fluid	E6a/b;A20	30	cT4N3M1	4	–	–	–
J-#928	F/71	Adenocarcinoma	Bronchial washing fluid	E6a/b;A20	0	cT4N3M1	4	ND	–	–
J-#996	M/52	Adenocarcinoma	Bronchial washing fluid	E6a/b;A20	0	cT3N3M0	3B	ND	–	–
J-#1001	F/32	Adenocarcinoma	Bronchial washing fluid	E13;A20	6.5	cT2N2M1	4	+	–	–

Abbreviations: F, female; M, male; NA, not available; ND, not determined.

CTGTGGAGGCTGAACTGGATC-3′ and 5′-TCATCAACAA-GCTCCACGGTG-3′) specific for the human ribonuclease P (RNase P) gene (GenBank accession number NM_005837). Given that we previously showed that the abundance of RNase P mRNA is similar to that of *EML4-ALK* mRNA in NSCLCs (data not shown), we used the successful amplification of RT-PCR products for RNase P as a threshold for selection of specimens for further analysis. Exclusion of small cell lung cancer specimens and filtering on the basis of RNase P mRNA abundance resulted in the isolation of 808 specimens of primary NSCLCs obtained from 754 individuals.

As shown in Supplementary Fig. S1, bronchial washing fluid, including bronchoalveolar lavage fluid and washing fluid for the brush, needle, forceps, and other implements used in bronchoscopy, constituted 66.3% of the 808 eligible samples, with the remaining specimens including pleural effusion (12.8%); surgically resected tumor (7.05%); sputum (4.33%); tumor biopsy tissue including that obtained by transbronchial lung biopsy and transbronchial needle aspiration (3.71%); peripheral blood (3.71%); cardiac effusion, spinal fluid, or ascites (1.36%); and metastatic lesions of NSCLCs (0.74%).

Multiplex RT-PCR analysis of EML4-ALK and KIF5B-ALK

Each specimen (with the exception of resected tumors) was mixed with an equal volume of RLT buffer at the Institute at which it was harvested. The resulting mixture was sent to Jichi Medical University, where DNA and RNA were extracted with the use of an automated BioRobot EZ1 workstation (Qiagen). The isolated RNA was subjected to RT with a ReverTra Ace qPCR RT kit (Toyobo), and the resulting cDNA was subjected to PCR for 50 cycles of incubation at 94°C for 15 seconds, 60°C for 30 seconds, and 72°C for 1 minute with AmpliTAQ Gold DNA polymerase (Applied Biosystems) and with 2 μmol/L of each of the following

Published OnlineFirst August 20, 2012; DOI: 10.1158/1078-0432.CCR-11-2947

primers: F-1, 5′-GCTTTCCCCGCAAGATGGACGG-3′; F-2, 5′-TACCAGTGCTGTCTCAATTGCAGG-3′; F-3, 5′-GTGCAGTGTTTAGCATTCTTGGGG-3′; F-4, 5′-AGCTACATCACACACCTTGACTGG-3′; F-5, 5′-TCAAGCACATCTCAAGAGCAAGTG-3′; F-6, 5′-ATCCTGCGGAACACTATTCAGTGG-3′; F-7, 5′-GACAGTTGGAGGAATCTGTCGATG-3′; F-8, 5′-CAGCTGAGAGAGTGAAAGCTTTGG-3′; and R-1, 5′-TCTTGCCAGCAAAGCAGTAGTTGG-3′. All PCR products were subjected to Sanger sequencing to confirm the presence of *EML4-ALK* or *KIF5B-ALK* cDNA.

Results

Multiplex RT-PCR system

In addition to the original *EML4-ALK* fusion cDNA in which exon 13 of *EML4* is fused to exon 20 of *ALK* in an in-frame manner (designated the E13;A20 variant by analogy with karyotype nomenclature; see http://atlasgeneticsoncology.org/Tumors/inv2p21p23NSCCLungID5667.html), 14 different variants of *EML4-ALK* have been described (1, 14, 21–27). Seven exons of *EML4* are theoretically capable of in-frame fusion with exon 20 of *ALK* (Fig. 1A), and all but the E1;A20 variant would be expected to produce an oncogenic EML4-ALK protein, given that the coiled-coil domain encoded by exon 2 is required for constitutive dimerization of EML4-ALK. In addition, 6 different exons of *KIF5B* are theoretically capable of in-frame fusion with exon 20 of *ALK* (Fig. 1A).

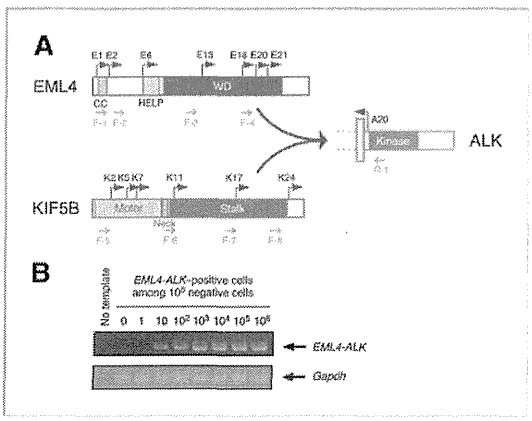

Figure 1. Multiplex RT-PCR system for detection of *EML4-ALK* and *KIF5B-ALK*. A, schematic representation of the structure of EML4, KIF5B, and ALK proteins. The positions of exons (E for *EML4* and K for *KIF5B*) theoretically capable of fusing in-frame to exon 20 (A20) of *ALK* are indicated by arrows. The positions of 8 forward primers (F-1 to F-8) and 1 reverse primer (R-1) for PCR are also indicated below the corresponding proteins. EML4 contains a coiled-coil domain (CC), a hydrophobic EMAP-like protein domain (HELP), and WD repeats (WD). KIF5B consists of an amino-terminal ATP-dependent motor domain, a neck region, and a stalk region. B, various numbers (0 to 1×10^6) of *EML4-ALK* (E13;A20)–positive BA/F3 cells (1) were mixed with a fixed number (1×10^6) of *EML4-ALK*–negative BA/F3 cells, and each mixture was analyzed with our multiplex RT-PCR system. A cDNA for mouse glyceraldehyde-3-phosphate dehydrogenase (*Gapdh*) was also amplified by PCR as an internal control with the primers 5′-TGTGTCCGTCGTGGATCTGA-3′ and 5′-CCTGCTTCACCACCTTCTTGA-3′.

To detect any such *EML4-ALK* or *KIF5B-ALK* fusion mRNAs, we developed a multiplex RT-PCR system. We had previously screened our archive of frozen tumors by RT-PCR analysis with 2 forward primers targeted to *EML4* and 1 reverse primer targeted to *ALK* (24), but such PCR conditions resulted in the amplification of products as large as ~1,300 bp for some variants. In this prospective study, we were faced with the analysis of a large number of samples with different levels of RNA quality. If the size of PCR products varied substantially among different *EML4-ALK* or *KIF5B-ALK* variants, some variants with large PCR products might not be amplified efficiently from specimens with low RNA quality. To be able to diagnose all possible fusions even with such samples, we therefore designed 4 forward primers for each of *EML4* and *KIF5B* so that the size variation among all possible RT-PCR products is minimal (Fig. 1A). This new multiplex system faithfully detected all known fusion variants from *EML4-ALK*–positive specimens in our previous archive of NSCLCs (data not shown).

To examine the sensitivity of our RT-PCR system, we mixed *EML4-ALK*–expressing BA/F3 cells (0 to 1×10^6) with *EML4-ALK*–negative cells (1×10^6) and then subjected them to RT-PCR analysis. A fusion cDNA was readily identified even with 10 positive cells (0.001%) among 1×10^6 negative cells (Fig. 1B), showing the high sensitivity of the RT-PCR system.

To confirm the potential of our RT-PCR–based system, we compared it with a sensitive immunohistochemical approach and with FISH for the diagnosis of our archive of surgically resected and freshly frozen tumors with high RNA quality. Fifteen NSCLC specimens that previously stained positive by our sensitive immunohistochemical approach, which is based on an intercalated antibody–enhanced polymer (iAEP) method (14), were analyzed by RT-PCR and FISH together with 96 iAEP-negative specimens in a blinded manner. RT-PCR analysis of all these specimens ($n = 111$) yielded a diagnosis identical to that obtained with the iAEP method ($P = 7.3 \times 10^{-19}$, Fisher exact test; data not shown). Analysis of the same sample set by a split FISH assay with Vysis probes (Abbott Laboratories) revealed that all of the iAEP-positive cases showed a rearranged *ALK* locus, whereas one iAEP-negative sample gave a discordant result (negative by iAEP and RT-PCR but positive by FISH; Supplementary Fig. S2). The reason for this discrepant result remains unclear, but the multiple signals obtained with the 3′-*ALK* probe in the FISH analysis are indicative of amplification of the *ALK* gene or its adjacent region. Despite this discrepancy, the RT-PCR and iAEP data were highly concordant with the FISH results ($P = 1.2 \times 10^{-17}$, Fisher exact test). Compared with the iAEP method, therefore, both the sensitivity and specificity of our RT-PCR system were 100%. In comparison with the Vysis FISH, the sensitivity and specificity of RT-PCR were 93.8% and 100%, respectively.

Detection of EML4-ALK

Screening of the 808 eligible specimens with our multiplex RT-PCR system identified positive products in 36 samples (4.46%) obtained from 32 different individuals

Published OnlineFirst August 20, 2012; DOI: 10.1158/1078-0432.CCR-11-2947

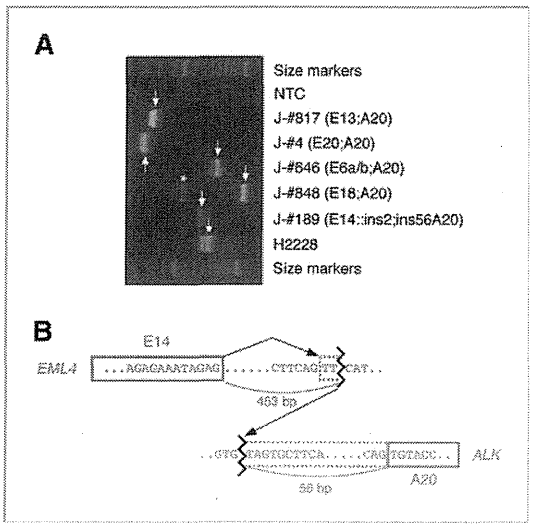

Figure 2. Multiplex RT-PCR detection of *EML4-ALK*–positive NSCLCs. A, RT-PCR products for each of the *EML4-ALK* variants identified in our cohort were separated by agarose gel electrophoresis. RT-PCR products spanning the *EML4-ALK* fusion points are indicated by arrows; the asterisk indicates a nonspecific product. An NSCLC cell line, H2228, harboring the E6a/b;A20 variant of *EML4-ALK* was used as a positive control for the PCR reaction. Size markers include a 50-bp DNA ladder (Invitrogen). NTC, no-template control. B, genomic structure of the fusion point for a novel variant of *EML4-ALK*. Nucleotide sequencing of the genomic PCR and RT-PCR products from patient J-#189 revealed that exon 14 of *EML4* (blue) was spliced to a TT sequence adjacent to the genomic ligation point, with transcription continuing in an in-frame manner into intron 19 and exon 20 of *ALK* (red).

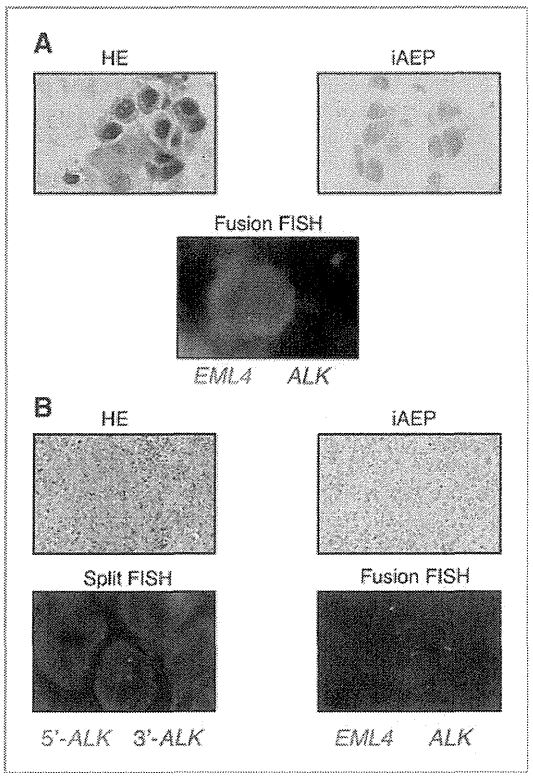

Figure 3. Specimens positive for *EML4-ALK* by RT-PCR but negative by iAEP-based IHC and by FISH. Sections of tumor biopsy specimens for J-#393 tumor (A) and J-#927 (B) were stained with hematoxylin-eosin (HE), subjected to immunohistochemical analysis by the iAEP method, and examined by split or fusion FISH. The color of fluorescence for the probes in each hybridization is indicated below the FISH images. Nuclei are stained blue with 4′,6-diamidino-2-phenylindole (DAPI).

(4.24%; Table 1, Fig. 2A). Nucleotide sequencing of each PCR product identified 19 cases positive for the E13;A20 variant, 10 cases for E6a/b;A20, a single case each for E18;A20, E20;A20, and a novel variant. *EML4-ALK* was detected in a wide range of specimens including bronchial washing fluid ($n = 11$), tumor biopsy ($n = 8$), resected tumor ($n = 7$), pleural effusion ($n = 5$), sputum ($n = 4$), and metastatic lymph node ($n = 1$). We did not detect any *KIF5B-ALK* cDNAs, confirming the rarity of this fusion gene.

Importantly, an E13;A20 product was consistently identified in both of the sputa obtained at different time points from patient J-#1. Likewise, an E13;A20 product was detected in both the tumor biopsy and sputum from patient J-#53 as well as in the pleural effusion and 2 resected tumor specimens from patient J-#330, supporting the reliability of our RT-PCR approach.

Sequence determination for the RT-PCR product from patient J-#189 revealed that exon 14 of *EML4* was fused to exon 20 of *ALK* with an intervening sequence. Genomic PCR analysis of the J-#189 specimen with a forward primer targeted to exon 14 of *EML4* and a reverse primer targeted to exon 20 of *ALK* yielded a specific product, nucleotide sequencing of which revealed that a position 453 bp downstream of *EML4* exon 14 was ligated to a position 56 bp upstream of *ALK* exon 20 (Fig. 2B). In the transcript of this fusion gene, exon 14 of *EML4* is thus spliced to a TT sequence that is located within *EML4* intron 14 and which is directly ligated to intron 19 of *ALK*. This splicing event results in an in-frame fusion between the mRNA sequences derived from *EML4* and *ALK*. Furthermore, a full-length cDNA for this variant, here designated E14::ins2;ins56A20, was isolated by RT-PCR analysis (Supplementary Fig. S3), and the potent transforming ability of the encoded protein was confirmed with an *in vitro* focus formation assay (Supplementary Fig. S4).

Comparison between multiplex RT-PCR and sensitive IHC

Finally, we applied the iAEP method to the *EML4-ALK*–positive cases for which FFPE specimens were also available ($n = 15$). All but 2 cases (J-#393 and J-#927) manifested clear immunoreactivity with antibodies to ALK (Table 1). FISH analysis of these 2 specimens also failed to detect the *EML4-ALK* rearrangements (Fig. 3). Given that genomic DNA was not available for the tumor of patient J-#393, we

Published OnlineFirst August 20, 2012; DOI: 10.1158/1078-0432.CCR-11-2947

were not able to determine whether the PCR result was a false-positive. For J-#927, however, PCR analysis of genomic DNA with a forward primer targeted to *EML4* exon 6 and a reverse primer to *ALK* exon 20 resulted in the amplification of an approximately 8.8-kbp genomic fragment, nucleotide sequencing of which revealed a fusion event between intron 6 of *EML4* and intron 19 of *ALK* (Supplementary Fig. S5). Isolation of the genomic fusion point thus indicates that J-#927 indeed harbors an *EML4-ALK*–positive tumor.

Discussion

We have conducted a large-scale, prospective screening for *EML4-ALK* with an RT-PCR–based approach. Whereas RNA extraction and cDNA synthesis add extra labor to the diagnostic procedure, certain introns of *EML4* are too large (intron 6 spans >16 kbp, for instance) for reliable amplification by genomic PCR. We therefore adopted RT-PCR as the method for our prospective screening. Specific PCR products were successfully isolated from different types of specimen, even from sputum (J-#1, J-#53, J-#215) and washing fluid of a tumor biopsy needle (J-#530). Multiple positive results obtained with different specimens of the same individuals further reinforce the reliability of our multiplex RT-PCR system as a diagnostic tool for *EML4-ALK*–positive tumors. Importantly, a subset of *EML4-ALK*–positive individuals diagnosed in the present study entered a clinical trial for crizotinib, and the response rate of the evaluable patients ($n = 9$) was 100% with this drug, again verifying the accuracy of our RT-PCR–based diagnosis.

The frequency of *EML4-ALK* in our cohort was 4.24% for all NSCLC cases and 6.11% for lung adenocarcinoma, values similar to those obtained in previous studies (20, 21). However, our prevalence data might be overestimates because the knowledge of mutual exclusiveness for *EML4-ALK* and *EGFR* mutations may have affected patient selection for our specimen collection. Indeed, *EGFR* mutation frequency among our cohort (23.8%) is slightly lower than that (30.9%) determined in a previous large-scale screening in Japan (28).

The clinicopathologic features of patients with *EML4-ALK*–positive tumors determined in the present study are also in agreement with those previously described, with a bias toward a young age, adenocarcinoma histology, and never or light smoking. Whereas a previous large-scale screening for *EML4-ALK* based on FISH did not detect a sex preference for the fusion gene (7), our cohort revealed a significant female preference. Such a sex difference was evident even among individuals below 40 years of age ($P = 0.03$, Fisher' exact test) and among those with an adenocarcinoma histology ($P = 0.005$, Fisher' exact test). Further large-scale studies are warranted to determine whether this uneven sex distribution of *EML4-ALK* is related to particular clinicopathologic features or ethnic groups.

Given that *EML4-ALK* and *EGFR* mutations are almost mutually exclusive and that the fusion gene is enriched in lung adenocarcinoma with an early onset, it should prove to be clinically beneficial to pay special attention to such subsets of patients. Indeed, *EML4-ALK* was detected in 27.7% of *EGFR* mutation–negative adenocarcinomas in individuals of younger than 50 years and in 50.0% of those in individuals of younger than 40 years in our cohort. Given the marked efficacy of ALK inhibitors in patients with *EML4-ALK*–positive NSCLCs (7), however, physicians should not dismiss the diagnosis in other subsets of patients. For example, *EML4-ALK* was even detected in an 80-year-old woman and in another woman with an intense smoking history (82 pack-years; Table 1).

Multiplex RT-PCR has both advantages and disadvantages compared with other techniques. Importantly, the accuracy of RT-PCR–based diagnosis depends markedly on the RNA quality of specimens. In our cohort, for instance, 71 (7.75%) of the initial 916 specimens were excluded from *EML4-ALK* screening because of a failure to obtain PCR products for RNase P (the other 37 samples were excluded because they were not NSCLCs). Low RNA quality thus clearly hampers reliable RT-PCR–based diagnosis.

Also, as expected, there was a large variation in the PCR cycle number required for successful amplification among specimens. In our cohort, 50 cycles of PCR allowed detection of PCR products for all positive cases, but such extensive amplification may also generate nonspecific products (as shown in Fig. 2A). Further optimization of primer sequences or combinations may minimize the generation of such byproducts. Furthermore, whereas our system should be able to capture all in-frame fusions of *ALK* to *EML4* or *KIF5B*, it is not capable in its present form of detecting *ALK* fusions to other partners, such as *KLC1-ALK*, which was recently shown to be present infrequently in NSCLCs (29).

On the other hand, RT-PCR can be readily applied to specimens such as sputum, bronchial washing fluid, or pleural effusion that may not be suitable for preparation of FFPE samples. Whereas the latter 2 specimen types can be used for the preparation of cell blocks suitable for analysis by FISH or IHC, this procedure may not be as widely adopted in the clinic as is FISH or IHC. More importantly, it is difficult to generate cell blocks or FFPE samples from sputum. Our current prospective screening identified 4 *EML4-ALK*–positive sputa of 35 samples (Table 1, Supplementary Fig. S1), showing that sputum is a suitable specimen for RT-PCR analysis. Indeed, sputum was the only available specimen from patient J-#215 both for the diagnosis of NSCLCs and for the detection of *EML4-ALK*. If RT-PCR had not been applied to this patient's sputum, we would not have been able to identify her tumor as positive for *EML4-ALK*, and she would not have had the chance to receive treatment with an ALK inhibitor in Japan.

Furthermore, PCR-based detection of *EML4-ALK* should have a higher analytic sensitivity compared with IHC or FISH (Fig. 1B). Even with sputum obtained from a patient with chronic bronchitis, RT-PCR was able to readily detect *EML4-ALK* at a concentration of 10 positive cells/mL (1). Thus, provided that RNA is not substantially degraded, RT-PCR–based diagnosis is expected to have a strong advantage

Published OnlineFirst August 20, 2012; DOI: 10.1158/1078-0432.CCR-11-2947

with regard to the detection of low numbers of *EML4-ALK*–positive cells.

Ideally, every NSCLC case should be examined for the presence of *EML4-ALK*, with a sensitive and accurate diagnostic strategy for the oncogenic fusion being essential for the adoption of ALK inhibitors in the clinic. Given the reliable detection of *EML4-ALK* mRNA by multiplex RT-PCR shown in the present study, we propose the following scheme for the comprehensive diagnosis of *EML4-ALK*–positive NSCLCs. For sputum, bronchial lavage fluid, pleural effusion, or other specimens that may not be suitable for the preparation of FFPE tissue, multiplex RT-PCR should be applied to detect *ALK* fusion mRNAs. In contrast, given that FFPE specimens usually have fragmented RNA, they should be subjected to FISH and to sensitive immunohistochemical analysis such as that described previously (14, 15). Furthermore, FISH or IHC can be applied to cell blocks prepared from some non-FFPE specimens. No single technique is therefore able to detect *EML4-ALK* in all types of specimen, and appropriate tests should be chosen on the basis of the specimens available for a given patient.

Disclosure of Potential Conflicts of Interest

H. Mano is the CEO of CureGene Co., Ltd.; has commercial research grant from Illumina, Inc. and Astellas Pharma Inc.; has ownership interest (including patents); and is on the consultant/advisory board of Chugai Pharmaceutical, Astellas Pharma Inc., and Daiichi Sankyo Co., Ltd. No potential conflicts of interest were disclosed by the other authors.

Authors' Contributions

Conception and design: K. Hagiwara, H. Mano
Development of methodology: K. Takeuchi, Y.L. Choi
Acquisition of data (provided animals, acquired and managed patients, provided facilities, etc.): M. Soda, K. Isobe, A. Inoue, S. Oizumi, Y. Fujita, A. Gemma, Y. Yamashita, K. Takeuchi, H. Miyazawa, T. Tanaka, K. Hagiwara
Analysis and interpretation of data (e.g., statistical analysis, biostatistics, computational analysis): M. Soda, T. Ueno, H. Mano
Writing, review, and/or revision of the manuscript: S. Oizumi, A. Gemma, K. Hagiwara, H. Mano
Administrative, technical, or material support (i.e., reporting or organizing data, constructing databases): M. Maemondo, K. Takeuchi, K. Hagiwara
Study supervision: H. Mano

Grant Support

This study was supported in part by a grant for Research on Human Genome Tailor-made from the Ministry of Health, Labor, and Welfare of Japan; by Grants-in-Aid for Scientific Research from the Ministry of Education, Culture, Sports, Science, and Technology of Japan; and by grants from the Japan Society for the Promotion of Science, from Takeda Science Foundation, from Mochida Memorial Foundation for Medical and Pharmaceutical Research, from The Mitsubishi Foundation, and from The Sagawa Foundation for Promotion of Cancer Research.

The costs of publication of this article were defrayed in part by the payment of page charges. This article must therefore be hereby marked *advertisement* in accordance with 18 U.S.C. Section 1734 solely to indicate this fact.

Received November 17, 2011; revised June 26, 2012; accepted August 3, 2012; published OnlineFirst August 20, 2012.

References

1. Soda M, Choi YL, Enomoto M, Takada S, Yamashita Y, Ishikawa S, et al. Identification of the transforming *EML4-ALK* fusion gene in non-small-cell lung cancer. Nature 2007;448:561–6.
2. Mano H. ALKoma: a cancer subtype with a shared target. Cancer Discov 2012;2:495–502.
3. Shaw AT, Solomon B. Targeting anaplastic lymphoma kinase in lung cancer. Clin Cancer Res 2011;17:2081–6.
4. Soda M, Takada S, Takeuchi K, Choi YL, Enomoto M, Ueno T, et al. A mouse model for *EML4-ALK*-positive lung cancer. Proc Natl Acad Sci U S A 2008;105:19893–7.
5. Chen Z, Sasaki T, Tan X, Carretero J, Shimamura T, Li D, et al. Inhibition of ALK, PI3K/MEK, and HSP90 in murine lung adenocarcinoma induced by EML4-ALK fusion oncogene. Cancer Res 2010;70:9827–36.
6. Marzec M, Kasprzycka M, Ptasznik A, Wlodarski P, Zhang Q, Odum N, et al. Inhibition of ALK enzymatic activity in T-cell lymphoma cells induces apoptosis and suppresses proliferation and STAT3 phosphorylation independently of Jak3. Lab Invest 2005;85:1544–54.
7. Kwak EL, Bang YJ, Camidge DR, Shaw AT, Solomon B, Maki RG, et al. Anaplastic lymphoma kinase inhibition in non-small-cell lung cancer. N Engl J Med 2010;363:1693–703.
8. Katayama R, Khan TM, Benes C, Lifshits E, Ebi H, Rivera VM, et al. Therapeutic strategies to overcome crizotinib resistance in non-small cell lung cancers harboring the fusion oncogene EML4-ALK. Proc Natl Acad Sci U S A 2011;108:7535–40.
9. Lovly CM, Heuckmann JM, de Stanchina E, Chen H, Thomas RK, Liang C, et al. Insights into ALK-driven cancers revealed through development of novel ALK tyrosine kinase inhibitors. Cancer Res 2011;71:4920–31.
10. Sakamoto H, Tsukaguchi T, Hiroshima S, Kodama T, Kobayashi T, Fukami TA, et al. CH5424802, a selective ALK inhibitor capable of blocking the resistant gatekeeper mutant. Cancer Cell 2011;19:679–90.
11. Gerber DE, Minna JD. ALK inhibition for non-small cell lung cancer: from discovery to therapy in record time. Cancer Cell 2010;18:548–51.
12. Butrynski JE, D'Adamo DR, Hornick JL, Dal Cin P, Antonescu CR, Jhanwar SC, et al. Crizotinib in ALK-rearranged inflammatory myofibroblastic tumor. N Engl J Med 2010;363:1727–33.
13. Mok TS, Wu YL, Thongprasert S, Yang CH, Chu DT, Saijo N, et al. Gefitinib or carboplatin-paclitaxel in pulmonary adenocarcinoma. N Engl J Med 2009;361:947–57.
14. Takeuchi K, Choi YL, Togashi Y, Soda M, Hatano S, Inamura K, et al. KIF5B-ALK, a novel fusion oncokinase identified by an immunohistochemistry-based diagnostic system for ALK-positive lung cancer. Clin Cancer Res 2009;15:3143–9.
15. Mino-Kenudson M, Chirieac LR, Law K, Hornick JL, Lindeman N, Mark EJ, et al. A novel, highly sensitive antibody allows for the routine detection of ALK-rearranged lung adenocarcinomas by standard immunohistochemistry. Clin Cancer Res 2010;16:1561–71.
16. Nagai Y, Miyazawa H, Huqun, Tanaka T, Udagawa K, Kato M, et al. Genetic heterogeneity of the epidermal growth factor receptor in non-small cell lung cancer cell lines revealed by a rapid and sensitive detection system, the peptide nucleic acid-locked nucleic acid PCR clamp. Cancer Res 2005;65:7276–82.
17. Shaw AT, Yeap BY, Mino-Kenudson M, Digumarthy SR, Costa DB, Heist RS, et al. Clinical features and outcome of patients with non-small-cell lung cancer who harbor EML4-ALK. J Clin Oncol 2009;27:4247–53.
18. Horn L, Pao W. EML4-ALK: honing in on a new target in non-small-cell lung cancer. J Clin Oncol 2009;27:4232–5.
19. Tiseo M, Gelsomino F, Boggiani D, Bortesi B, Bartolotti M, Bozzetti C, et al. EGFR and EML4-ALK gene mutations in NSCLC: a case report of erlotinib-resistant patient with both concomitant mutations. Lung Cancer (Amsterdam, the Netherlands) 2011;71:241–3.
20. Inamura K, Takeuchi K, Togashi Y, Hatano S, Ninomiya H, Motoi N, et al. EML4-ALK lung cancers are characterized by rare other mutations, a TTF-1 cell lineage, an acinar histology, and young onset. Mod Pathol 2009;22:508–15.
21. Wong DW, Leung EL, So KK, Tam IY, Sihoe AD, Cheng LC, et al. The EML4-ALK fusion gene is involved in various histologic types of lung

Published OnlineFirst August 20, 2012; DOI: 10.1158/1078-0432.CCR-11-2947

cancers from nonsmokers with wild-type EGFR and KRAS. Cancer 2009;115:1723–33.
22. Choi YL, Takeuchi K, Soda M, Inamura K, Togashi Y, Hatano S, et al. Identification of novel isoforms of the *EML4-ALK* transforming gene in non-small cell lung cancer. Cancer Res 2008;68:4971–6.
23. Koivunen JP, Mermel C, Zejnullahu K, Murphy C, Lifshits E, Holmes AJ, et al. EML4-ALK fusion gene and efficacy of an ALK kinase inhibitor in lung cancer. Clin Cancer Res 2008;14:4275–83.
24. Takeuchi K, Choi YL, Soda M, Inamura K, Togashi Y, Hatano S, et al. Multiplex reverse transcription-PCR screening for *EML4-ALK* fusion transcripts. Clin Cancer Res 2008;14:6618–24.
25. Lin E, Li L, Guan Y, Soriano R, Rivers CS, Mohan S, et al. Exon array profiling detects EML4-ALK fusion in breast, colorectal, and non-small cell lung cancers. Mol Cancer Res 2009;7:1466–76.
26. Takahashi T, Sonobe M, Kobayashi M, Yoshizawa A, Menju T, Nakayama E, et al. Clinicopathologic features of non-small-cell lung cancer with EML4-ALK fusion gene. Ann Surg Oncol 2010;17:889–97.
27. Sanders HR, Li HR, Bruey JM, Scheerle JA, Meloni-Ehrig AM, Kelly JC, et al. Exon scanning by reverse transcriptase-polymerase chain reaction for detection of known and novel EML4-ALK fusion variants in non-small cell lung cancer. Cancer Genet 2011;204:45–52.
28. Toyooka S, Matsuo K, Shigematsu H, Kosaka T, Tokumo M, Yatabe Y, et al. The impact of sex and smoking status on the mutational spectrum of epidermal growth factor receptor gene in non small cell lung cancer. Clin Cancer Res 2007;13:5763–8.
29. Togashi Y, Soda M, Sakata S, Sugawara E, Hatano S, Asaka R, et al. KLC1-ALK: a novel fusion in lung cancer identified using a formalin-fixed paraffin-embedded tissue only. PLoS One 2012;7:e31323.

Published OnlineFirst August 20, 2012; DOI: 10.1158/1078-0432.CCR-11-2947

AACR American Association for Cancer Research

Clinical Cancer Research

A Prospective PCR-Based Screening for the *EML4-ALK* Oncogene in Non–Small Cell Lung Cancer

Manabu Soda, Kazutoshi Isobe, Akira Inoue, et al.

Clin Cancer Res 2012;18:5682-5689. Published OnlineFirst August 20, 2012.